
Training CNNs faster with Dynamic Input and Kernel Downsampling

Zissis Poulos

Department of Electrical and Computer Engineering
University of Toronto
Toronto, CA
zpoulos@eecg.toronto.edu

Ali Nouri

Department of Electrical and Computer Engineering
University of Toronto
Toronto, CA
ali.nouri@mail.utoronto.ca

Andreas Moshovos

Department of Electrical and Computer Engineering
University of Toronto
Toronto, CA
moshovos@eecg.toronto.edu

Abstract

We reduce training time in convolutional networks (CNNs) with a method that, for some of the mini-batches: a) scales down the resolution of input images via downsampling, and b) reduces the forward pass operations via pooling on the convolution filters. Training is performed in an interleaved fashion; some batches undergo the regular forward and backpropagation passes with original network parameters, whereas others undergo a forward pass with pooled filters and downsampled inputs. Since pooling is differentiable, the gradients of the pooled filters propagate to the original network parameters for a standard parameter update. The latter phase requires fewer floating point operations and less storage due to the reduced spatial dimensions in feature maps and filters. The key idea is that this phase leads to smaller and approximate updates and thus slower learning, but at significantly reduced cost, followed by passes that use the original network parameters as a refinement stage. Deciding how often and for which batches the downsampling occurs can be done either stochastically or deterministically, and can be defined as a training hyperparameter itself. Experiments on residual architectures show that we can achieve up to 23% reduction in training time with minimal loss in validation accuracy.

1 Introduction

The abundance of large annotated image datasets has sparked a boom in the applicability of convolutional neural networks (CNNs) on visual tasks, but it also necessitates developing and prototyping large capacity models to capture complex input distributions. This capacity increase comes with much higher demands in terms of training resources. The computational and data footprint cost of state-of-the-art CNN models may exceed billions of floating-point operations (FLOPs) and dozens

of gigabytes (GBs), respectively, especially in a mini-batch setting, which is the most common mode of operation when training such models [He et al., 2016, He et al., 2016, Szegedy et al., 2017, Krizhevsky et al., 2017].

Distributing the process is one straightforward approach to handle the vast size of the compute and peak memory encountered during training [Vanhoucke et al., 2011]. Training is split into sub-tasks, usually by partitioning input batches. Then, training on these partitions is delegated as separate processes to multiple cluster nodes, be it multiple graphics processing units (GPUs) or custom hardware (e.g. ASICs). Such approaches however obligate that large multi-core and/or multi-GPU systems are available on demand, which is not always the case. Particularly in prototyping stages, model architectures rapidly change and hyperparameters are tuned to determine what model instance will eventually be deployed. Therefore, evaluating whether training converges to acceptable accuracy levels -or if learning even takes place- must happen in short cycles and ideally without the need to utilize large compute platforms. Moreover, distributed training ideally requires extremely large batch sizes to fully utilize cluster nodes. However, arbitrarily increasing the batch size may jeopardize or stall convergence, and therefore batches are in practice reduced in size, effectively limiting the number of cluster nodes that can be utilized [Gupta et al., 2017, Krizhevsky, 2014].

Consequently, a long thread of research is devoted to reducing the cost of training by viewing the problem from an algorithmic or model-level perspective, irrespective of the hardware platform(s) invoked for training. The major challenge that these methods face is preserving the representational capacity of a target architecture, while reducing training time. We can broadly categorize these methods based on the property they target towards reducing total training time: a) fast convergence methods, and b) per-iteration compute/memory reduction methods. We note that methods between these two categories can often be combined to attain cumulative benefits.

Fast convergence: These methods focus on achieving faster convergence and they effectively reduce the number of iterations (or epochs) required to reach or surpass state-of-the-art accuracy in various datasets. In this context, batch-normalization is a widely adopted method that maintains the stability of feature extraction distributions across layers, allowing deeper architectures with good convergence rates [Ioffe and Szegedy, 2015]. More recently, it was empirically discovered that estimating optimal learning rates on-the-fly and applying those during training instead of using the fixed training policies that are traditionally used, can cause some models to converge extremely fast; a phenomenon coined *super-convergence* [Smith and Topin, 2017]. Finally, knowledge transfer has been proposed as a method to convey the parameters of a small network to a deeper and/or wider model instance via function preserving transformations [Chen et al., 2016]. This allows learning in the larger model to commence with initial parameters that would otherwise be learned with much more expensive iterations during the first epochs of training.

Per-iteration compute/memory reduction: Early techniques in this category reduce the number of FLOPs per iteration, either with more efficient implementations of the convolution operation [Lavin, 2015, Mathieu et al., 2014], or by introducing low-rank approximations of the convolution kernels that enable cost-efficient computations [Jaderberg et al., 2014]. Another class of methods performs weight pruning or quantization during training reducing the number of multiplications in the forward and backward passes, the number of weight updates and storage requirements as well [Lym et al., 2019, Alvarez and Salzmann, 2016]. More recent methods apply transformations to the target architecture that downsample the feature maps and/or the convolution filters to reduce execution time early in the training phase and eventually resize those to the dimensions required by the target architecture towards later epochs [de Gusmão et al., 2016].

Related techniques have also been applied for reducing the inference cost of deployed models and are applicable when inference is performed in resource-constrained environments (limited compute and/or memory bandwidth) [Kuen et al., 2018, Tan and V. Le, 2019, Teerapittayanon et al., 2016].

Despite being successful in reducing CNN training time, several of these methods may require that some desirable properties of the training process or the target architecture itself are sacrificed. Specifically, pruning and quantization methods almost always cause degradation in validation accuracy compared to the baseline networks [Lym et al., 2019, Alvarez and Salzmann, 2016]. Techniques for reduced-cost implementation of convolution operations maximize their efficacy when kernels are generally large or the mini-batch size is relatively small, which limits the ability to explore various architectures and the hyperparameter space [Lavin, 2015, Mathieu et al., 2014]. Knowledge transfer methods, on the other hand, do not impose such limitations, but they do require training multiple

smaller instances of a target architecture, constructing a pool of such trained models (or require that it exists *a priori*), and selecting the one that performs best to transplant its weights to the larger model [Chen et al., 2016]. Finally, existing downsampling methods use heuristics to determine the downsampling factor when resizing convolution kernels and apply fixed spatial scaling to upsample back to the original shape [de Gusmão et al., 2016]. This process is inherently lossy in terms of accuracy and spatial resolution and thus constrains the applicability of these transformations; they must be applied only during early stages of training so that enough time is available to recuperate from any accuracy loss. In turn, this limits gains regarding total training time, despite the fact that these transformations can dramatically reduce FLOPs per iteration.

In this work, we overcome some of the above limitations with a method that: a) enables a significant portion of the training iterations to be performed at very low-cost (measured in FLOPs), b) can apply these iterations during early and late epochs in the training phase, c) requires no pre-training on a separate smaller instance of the target architecture, and d) does not degrade validation accuracy. A low-cost iteration is formed by downsampling the input images of the corresponding mini-batch and all the convolution kernels involved in the forward pass. The key novelty behind the proposed formulation is that kernel downsampling is done via differentiable transformations on the kernels of the target architecture. Differentiable transformations allow gradients of the downsampled kernels to propagate backwards to the target architecture’s parameters without lossy rescaling. Essentially, we learn parameter updates for the target architecture indirectly, using the downsampled kernels as representative samples for the forward pass computation, requiring much fewer FLOPs for inference and gradient computation. This permits us to apply these transformations more aggressively at various epochs during training and interleave them with iterations that use the original shape kernels and full resolution images. Experiments on CIFAR-10 and CIFAR-100 datasets with residual architectures show that we can achieve up to 31% reduction in training time with no loss in validation accuracy.

2 Methodology

There is a twofold rationale behind the proposed approach to reduce training costs. First, a down-sampled image tends to convey similar input features compared to its full resolution counterpart and it preserves most of the necessary input information for classification tasks [Chrabaszcz et al., 2017]. Pre-training on downsampled images followed by transfer learning to full resolution datasets is common in literature [Chen et al., 2016, Hinton et al., 2015]. Of course, aggressive downsampling may remove some of the distinctive features of the full resolution image (*e.g.*, blurred edges, merged image blobs) and cause accuracy deterioration, thus it needs to be done cautiously. Second, for a downsampled image the pixel neighborhood that captures parts of image content useful to classification is proportionally smaller than the neighborhood that captures the same content in the full resolution image. That is, if an input image x with dimensions $H \times W \times D$ is downsampled with a ratio of r (some divisor of H and W other than 1) to produce a lower resolution image \hat{x} with dimensions $(H/r) \times (W/r) \times D$, then a $K \times K \times D$ input volume in x is represented by a $(K/r) \times (K/r) \times D$ volume in \hat{x} . Therefore, we posit that reducing the receptive field of convolution filters also by a factor of (approximately) r per dimension is reasonable and can further reduce the number of operations. The transformation that is applied on filter weights to achieve this reduction is of course of paramount importance towards preserving the intended feature extraction capability of the original filters.

This spatial correlation between downsampled inputs and convolution kernels can be exploited to reduce the computation during a forward pass, either for a single input image or for a mini-batch. When fewer parameters and activations are involved in the forward computation, then the compute and storage requirements of the backpropagation algorithm are also reduced. In what follows we describe a method to perform such low-cost training iterations. When the network performs a low-cost iteration we refer to it as *low-mode* operation. On the other hand, when the kernel and input shapes are unmodified we say that the network is in *full-mode* operation.

2.1 Full-mode Operation

In full-mode, the network performs all computations that are dictated by its specification. We restrict our attention to convolutional layers, since these usually dominate execution time and are the ones that this method modifies dynamically during the training process.

Given an input image I let function $\mathbf{y} = f(I; \boldsymbol{\theta})$ represent the network in full-mode operation, where I is the input image, \mathbf{y} is the output of the network which is a distribution of conditional probabilities over class categories given I , and $\boldsymbol{\theta}$ is the collection of the network’s learnable parameters (or weights). Also, let $\mathbf{h}^{(i)} = \phi(\mathbf{W}^{(i)}\mathbf{h}^{(i-1)})$ represent convolutional layer i in full-mode, where $\mathbf{h}^{(i-1)}$ is an input tensor of activations to the layer, $\mathbf{W}^{(i)}$ is the weight matrix, ϕ is an activation function (e.g., ReLU), and $\mathbf{h}^{(i)}$ is the output tensor of activations.

To derive an asymptotic cost for convolutional layer i , let the dimensions of the input activation tensor be such that $\mathbf{h}^{(i-1)} \in \mathbb{R}^{H^{(i-1)} \times W^{(i-1)} \times C^{(i-1)}}$, where $H^{(i-1)}$, $W^{(i-1)}$ and $C^{(i-1)}$ denote the height, width and channel depth, respectively. If the first layer of the network ($i = 1$) is a convolutional layer then we have $\mathbf{h}^{(0)} \equiv I$, with $I \in \mathbb{R}^{H \times W \times C}$. Finally, the weight matrix $\mathbf{W}^{(i)}$ can be represented as a collection of $N^{(i)}$ kernels (or filters) of size $K^{(i)} \times K^{(i)} \times C^{(i-1)}$, each of which is convolved with $\mathbf{h}^{(i-1)}$ to produce a single output activation in $\mathbf{h}^{(i)}$. The asymptotic complexity of layer i can then be written as $\mathcal{O}((K^{(i)})^2 C^{(i-1)} H^{(i)} W^{(i)} C^{(i)})$.

In practice, it is common to train a CNN in a mini-batch setting, where forward computation is performed in batches of input images. In each training iteration t , the network accepts a batch of input images denoted $\mathbf{B}_t = \{I_1, \dots, I_{|\mathbf{B}_t|}\}$. Updating the network’s parameters after iteration t is related to the following minimization:

$$\min_{\boldsymbol{\theta}_t} L(\boldsymbol{\theta}_t) \tag{1}$$

$$L(\boldsymbol{\theta}_t) = \frac{1}{|\mathbf{B}_t|} \sum_{j=1}^{|\mathbf{B}_t|} L(t_j, f(I_j; \boldsymbol{\theta}_t))$$

where $L(t_j, f(I_j; \boldsymbol{\theta}_t))$ is the loss function quantifying the error between the ground truth label t_j of input I_j and the network’s output $f(I_j; \boldsymbol{\theta}_t)$ when the network’s parameters in iteration t are $\boldsymbol{\theta}_t$. The backpropagation algorithm is then applied to compute gradient updates for all network parameters [Rumelhart et al., 1988]. Here, we focus again on the update step for convolutional layer i . Suppose that $\mathbf{W}_{t-1}^{(i)}$ is the weight matrix of layer i at the end of iteration $t - 1$ (beginning of iteration t). Then, the weight matrix is updated to $\mathbf{W}_t^{(i)}$ using the steepest gradient descent method, as follows:

$$\mathbf{W}_t^{(i)} \leftarrow \mathbf{W}_{t-1}^{(i)} - \epsilon \frac{\partial L(\mathbf{W}_{t-1}^{(i)})}{\partial \mathbf{W}_{t-1}^{(i)}} \tag{2}$$

where $L(\boldsymbol{\theta}_{t-1})$ is the cost to minimize over mini-batch \mathbf{B}_t , and ϵ is the learning rate.

2.2 Low-mode Operation

In low-mode operation we force the network to perform a forward pass at a drastically decreased cost by: a) reducing the spatial dimensions of the input images and b) reducing the spatial dimensions of the kernels in each convolutional layer i . We note that the number of channels $C^{(i-1)}$ of the input activations and the number of filters $N^{(i)}$ remain unchanged in this mode.

2.2.1 Input Downsampling

We use $\hat{I} \stackrel{r}{\leftarrow} I$ to denote that image $I \in \mathbb{R}^{H \times W \times C}$ is downsampled to image $\hat{I} \in \mathbb{R}^{(H/r) \times (W/r) \times C}$ with a ratio r per dimension, where r is some divisor of H and W other than 1. This spatial transformation can be performed with various techniques, including Gaussian blurring followed by row/column elimination, or bi-linear interpolation [Nixon and Aguado, 2008]. We give preference to the former since it behaves well for $r > 2$. The notation implicitly applies when we refer to batches of images, and in that case we use $\hat{\mathbf{B}}_t \stackrel{r}{\leftarrow} \mathbf{B}_t$ to say that all images in batch $\mathbf{B}_t = \{I_1, \dots, I_{|\mathbf{B}_t|}\}$ are downsampled by a ratio of r to create batch $\hat{\mathbf{B}}_t = \{\hat{I}_1, \dots, \hat{I}_{|\hat{\mathbf{B}}_t|}\}$.

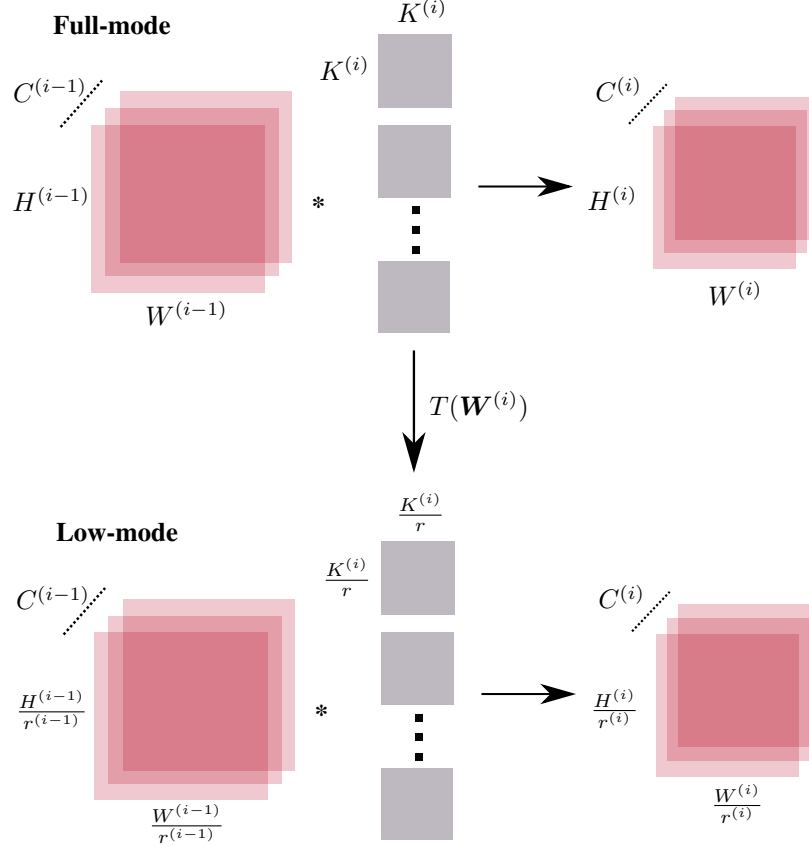


Figure 1: Full-mode vs. Low-mode forward computation for a convolutional layer

2.2.2 Kernel Downsampling

Given a kernel $\mathbf{F}^{(i)}$ in layer i with size $K^{(i)} \times K^{(i)} \times C^{(i-1)}$ we create kernel $\hat{\mathbf{F}}^{(i)}$ with dimensions $\lceil K^{(i)}/r \rceil \times \lceil K^{(i)}/r \rceil \times C^{(i-1)}$ using a *differentiable* spatial transformation $T(\cdot)$, so that $T(\mathbf{F}) = \hat{\mathbf{F}}$. We have experimented with various transformations, observing different effects in accuracy. The transformation we propose is an average pooling operator that produces filters with odd dimensions. For example, if $r = 2$ and \mathbf{F} is a $5 \times 5 \times C$ filter then $\hat{\mathbf{F}} = T(\mathbf{F}) = \text{AvgPool}(\mathbf{F})$, where $\text{AvgPool}(\cdot)$ is a 2×2 pooling operator with stride 2 and asymmetric padding. The resulting filter $\hat{\mathbf{F}}$ has dimensions $3 \times 3 \times C$. Alternatively we can generate $\lfloor K/r \rfloor \times \lfloor K/r \rfloor \times C$ filters, depending on the architecture. Indicatively, we use 3×3 average pooling to transform 3×3 convolutions to 1×1 pointwise convolutions.

Downsampling both input and convolution kernels may cause a cascading effect of spatially reduced feature maps in intermediate layers. The ratio of this (indirect) downsampling for input activations can be controlled through the stride parameter. Suppose that in low-mode, the input activations of layer i are $\hat{\mathbf{h}}^{(i-1)} \in \mathbb{R}^{H^{(i-1)}/r^{(i-1)} \times W^{(i-1)}/r^{(i-1)} \times C^{(i-1)}}$, where $r^{(i-1)}$ is the reduction factor compared to the spatial dimensions of the full-mode activation inputs $\mathbf{h}^{(i-1)}$. An analogous reduction can be obtained for the output activations as well, so that these become $\hat{\mathbf{h}}^{(i)} \in \mathbb{R}^{H^{(i)}/r^{(i)} \times W^{(i)}/r^{(i)} \times C^{(i)}}$.

The asymptotic complexity of layer i in low-mode can then be expressed as $\mathcal{O}((K^{(i)}/r)^2 C^{(i-1)} (H^{(i)}/r^{(i)}) (W^{(i)}/r^{(i)}) C^{(i)})$. In a relative sense, the low-mode operation for layer i involves $\mathcal{O}((r)^2 (r^{(i)})^2)$ less computation compared to the full-mode operation.

3 Learning in Low-mode

With these transformations the network now computes some function $\hat{\mathbf{y}} = \hat{f}(\hat{\mathbf{I}}; \hat{\boldsymbol{\theta}})$, where $\hat{\mathbf{y}} \neq \mathbf{y}$, in general, and $\hat{\boldsymbol{\theta}}$ is the new set of (transformed) parameters. For clarity we can use the transformation $T(\cdot)$ on $\boldsymbol{\theta}$ to mean that the relevant parameters (convolution weights) are transformed to generate $\hat{\boldsymbol{\theta}}$. That is, we write $\hat{\boldsymbol{\theta}} = T(\boldsymbol{\theta})$. Similarly, we say that $\hat{\mathbf{W}}^{(i)} = T(\mathbf{W}^{(i)})$ is the weight matrix of the transformed parameters for layer i , *i.e.* the collection of all $N^{(i)}$ downsampled kernels of layer i after applying the transformation $T(\cdot)$ with downsampling ratio r . The goal then at iteration t , if it is performed in low-mode, is to minimize:

$$\min_{\boldsymbol{\theta}_t} \mathbf{L}(T(\boldsymbol{\theta}_t)) \tag{3}$$

$$\mathbf{L}(T(\boldsymbol{\theta}_t)) = \frac{1}{|\hat{\mathbf{B}}_t|} \sum_{j=1}^{|\hat{\mathbf{B}}_t|} \mathbf{L}(t_j, \hat{f}(\hat{\mathbf{I}}_j; T(\boldsymbol{\theta}_t)))$$

If iteration t occurs in low-mode, let $\hat{\mathbf{W}}_{t-1}^{(i)}$ be the weight matrix of the transformed parameters for layer i at the beginning of iteration t . Then, layer i computes some non-linear function $\hat{\mathbf{h}}^{(i)} = \phi(\hat{\mathbf{W}}_{t-1}^{(i)} \hat{\mathbf{h}}^{(i-1)})$. The gradients of $\hat{\mathbf{W}}_{t-1}^{(i)}$ with respect to the loss in Eq.3, $\partial \mathbf{L}(\hat{\mathbf{W}}_{t-1}^{(i)}) / \partial \hat{\mathbf{W}}_{t-1}^{(i)}$, are computed by backpropagation as usual. The end goal, however, is to derive updates for weight matrix $\mathbf{W}^{(i)}$; that is, the network parameters before the application of $T(\cdot)$, so that these can be used during subsequent full-mode operations. If $T(\cdot)$ is selected such that it is differentiable everywhere (*e.g.*, average pooling as previously discussed), then $\partial \hat{\mathbf{W}}_{t-1}^{(i)} / \partial \mathbf{W}_{t-1}^{(i)} = \partial T(\mathbf{W}_{t-1}^{(i)}) / \partial \mathbf{W}_{t-1}^{(i)}$ exists and can be used to compute updates for $\mathbf{W}_t^{(i)}$ by an additional step of the backpropagation algorithm:

$$\mathbf{W}_t^{(i)} \leftarrow \mathbf{W}_{t-1}^{(i)} - \epsilon \frac{\partial \mathbf{L}(\hat{\mathbf{W}}_{t-1}^{(i)})}{\partial \hat{\mathbf{W}}_{t-1}^{(i)}} \frac{\partial \hat{\mathbf{W}}_{t-1}^{(i)}}{\partial \mathbf{W}_{t-1}^{(i)}} \tag{4}$$

3.1 Selecting Low-mode Iterations

Choosing which iterations and how many are done in low-mode is expected to affect the convergence rate of the target architecture. Aggressive policies where many contiguous iterations are on downsampled inputs and kernels may cause severe deterioration in accuracy, from which the model may fail to recover. In contrast, overly pessimistic policies where low-mode iterations are infrequent may produce negligible runtime benefits.

In this work, we adopt a stochastic scheme where the model alternates between the two modes with some pre-specified probability, determined before training commences. Specifically, we define p_{low}^e to be the probability that the next iteration is done in low-mode within epoch e (the probability may differ across epochs). For instance, assuming that training is divided into E epochs, then setting $p_{low}^e = 0.5, 1 \leq e \leq E$ forces the model into low-mode half of the time *in expectation*. However, we found that letting the target model operate in full-mode for the first few epochs after a learning rate adjustment takes place helps with fast convergence and accuracy refinement, respectively. Details are further discussed in Section 4. The policy can also be deterministic (*e.g.*, alternating based on a fixed frequency), but we give preference to stochastic schemes to remove any bias that a deterministic policy may introduce.

3.2 Overall Training Algorithm

The pseudocode for training a target model M using the method presented here (with downsampling ratio r), is given below. We assume that the per-epoch low-mode probabilities are determined beforehand and gathered into a vector P of length E .

In the process outlined above, the generation of downsampled images (Line 10) can also be done off-line for the entire training set as long as one ensures batches B_t and \hat{B}_t match after each shuffling

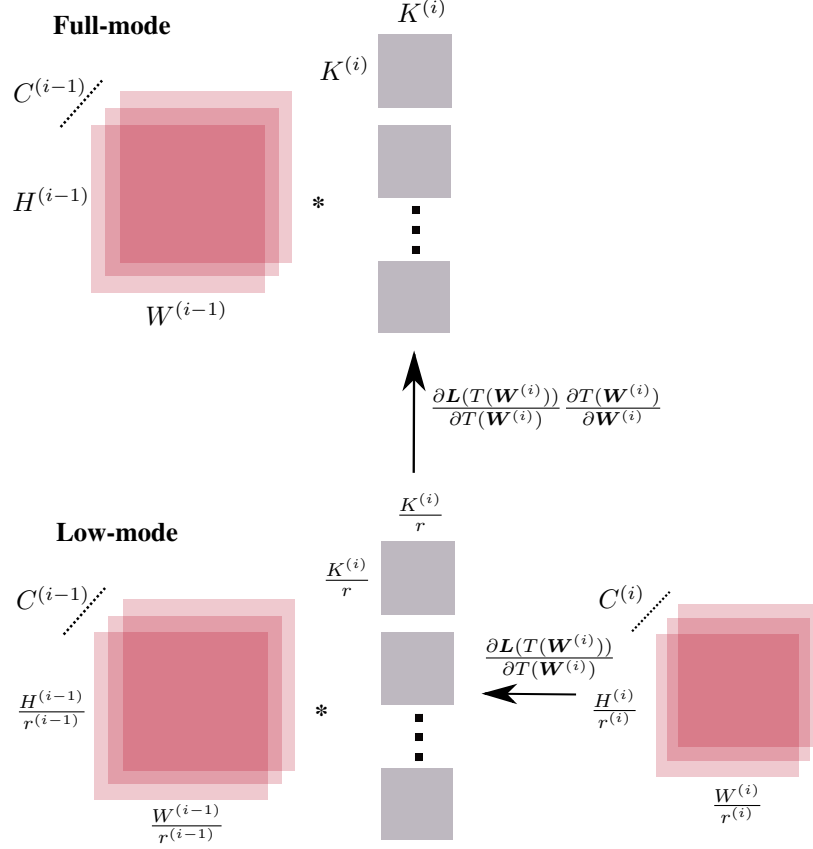


Figure 2: Low-mode backward propagation for convolutional layer weights $\mathbf{W}^{(i)}$

Algorithm 1 Training with Downsampling

- 1: **Input:** model M , downsampling ratio r , per-epoch downsampling probabilities P
 - 2: **for** $e = 1 : E$ **do**
 - 3: $p_{low}^e \leftarrow P[e]$
 - 4: **for** $t = 1 : T$ **do**
 - 5: $low \leftarrow \text{Bernoulli}(p_{low}^e)$
 - 6: **if** $low == 0$ **then**
 - 7: train model M with batch \mathbf{B}_t , kernels $\mathbf{F}^{(i)}$ for all convolution layers i
 - 8: update $\boldsymbol{\theta}_t$
 - 9: **if** $low == 1$ **then**
 - 10: $\hat{\mathbf{I}}_k \xleftarrow{r} \mathbf{I}_k, \forall \mathbf{I}_k \in \mathbf{B}_t$,
 - 11: $\hat{\mathbf{B}}_t \xleftarrow{r} \mathbf{B}_t$
 - 12: $\hat{\mathbf{W}}_{t-1}^{(i)} = T(\mathbf{W}_{t-1}^{(i)})$ with ratio r for all convolution layers i
 - 13: train model M with batch $\hat{\mathbf{B}}_t$, parameters $\hat{\mathbf{W}}_{t-1}^{(i)}$ for all convolution layers i
 - 14: update $\mathbf{W}_t^{(i)}$ using Eq.4 for all convolution layers i
-

round between epochs. The transformation can be applied on the host side (CPU) in the case where GPUs are used for training, thus it does not have to consume processing time on the device side. The weight transformations (Line 12) are performed on the device side during the forward pass. Finally, in the pseudocode we suppress the update of weights for fully connected (FC) layers (it is explicit in Line 8 and implied in Line 14), since FC parameters are shared between the two modes of operation.

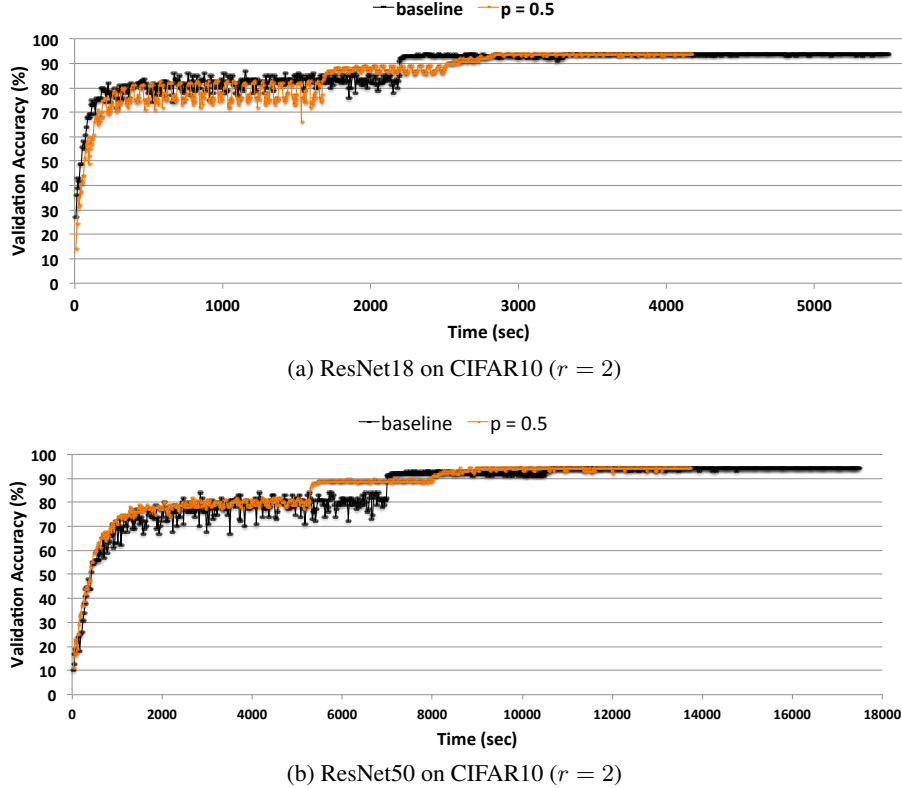


Figure 3: Validation accuracy vs. time, between baseline training and the proposed method

4 Experiments

We evaluate the proposed method on the residual architectures ResNet18 and ResNet50 [He et al., 2016, He et al., 2016] using the CIFAR10 dataset [Krizhevsky, 2012]. We measure runtime on an NVIDIA 1080Ti GPU. A summary of the experimental setting is given below:

1. Downsampling ratio $r = 2$ (*i.e.*, input images have dimensions $16 \times 16 \times 3$ in low-mode).
2. Total number of epochs $E = 200$, and batch size $|B_t| = |\hat{B}_t| = 125$.
3. Full-mode / Low-mode: we let the first 4 epochs immediately after a learning rate adjustment to run on full-mode exclusively ($p_{low}^e = 0$). In the residual models studied, learning rate begins at 0.1 and is adjusted to 0.01 at epoch 80 and to 0.001 at epoch 120 [He et al., 2016, He et al., 2016].
4. The downsampling probability is set to $p_{low}^e = p = 0.5$ for all other epochs.
5. Due to the fact that feature maps have reduced spatial dimensions through all layers in low-mode, we drop the max pooling layer immediately after the first convolutional layer in both ResNet18 and ResNet50 (only in low-mode).
6. ResNet18: the 3×3 kernels in layers conv1 and conv2 of the basic block cell are transformed to 1×1 kernels as per Section 3.
7. ResNet50: only the 3×3 kernels in layer conv2 of the bottleneck cell are transformed to 1×1 kernels.
8. FC layers remain unchanged in both models.
9. Other hyper-parameters remain unchanged, including kernel strides and optimizer parameters, such as momentum and weight decay [He et al., 2016, He et al., 2016].

Figure 3 illustrates the validation accuracy curves achieved on the two models studied when the proposed downsampling method is applied using the setting above. We compare those to the validation

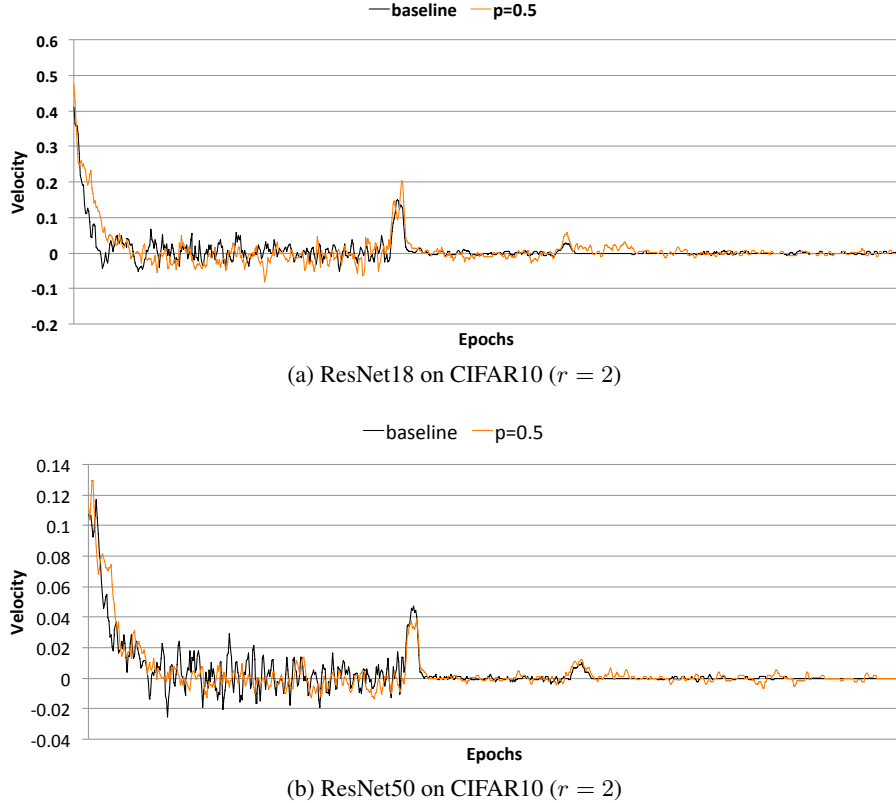


Figure 4: Velocity per epoch, between baseline training and the proposed method

curves of the standard training process, referred to as *baseline* in the figure. For the proposed method and the baseline we apply the same training hyper-parameters (summarized above), and in fact ensure that they match the suggested ones in the original publications of these models [He et al., 2016, He et al., 2016]. The figures plot accuracy over time, which includes GPU time accounting for both forward and backward passes and host time for transforming the input images.

The extent of the proposed method’s success can be based on two criteria: a) whether it converges to the same validation accuracy as the baseline, and b) whether the validation curve is time-shifted to the left, *i.e.* convergence to the final (maximum) accuracy is achieved earlier in the proposed method. As Figure 3(a) shows, the proposed method on ResNet18 (with downsampling probability $p = 0.5$) converges to 94% accuracy at around 2,800 seconds (≈ 47 minutes), while the baseline method hits the same accuracy levels at 3,400 seconds (≈ 57 minutes). This constitutes an 18% reduction in runtime. For a deeper and larger capacity model however, such as ResNet50, runtime gains are more pronounced. As shown in Figure 3(b), downsampling on ResNet50 with $p = 0.5$ leads to the same accuracy as the baseline, but does so 23% faster (≈ 150 vs. ≈ 193 minutes). Faster convergence in ResNet50 vs. ResNet18 (in a relative sense) cannot be merely attributed to compute reduction per-layer in low-mode operation; these are similar between the two models. Indicatively, a single iteration during low-mode consumes 39% of a full-mode iteration in ResNet50 and 37% in ResNet18. Thus, this behavior could instead rise from the robustness of the deeper architecture: the deeper architecture is expected to be less sensitive to the weight transformations in low-mode (less likely to observe a drop in accuracy) and can also recover better from any loss if it occurs.

To illustrate this phenomenon, Figure 4 demonstrates how learning progresses for ResNet18 and ResNet50 when the proposed downsampling method is applied. Specifically, learning progress is quantified by measuring the velocity of training and how this changes throughout epochs. Here, velocity is the quotient $\frac{\Delta A}{\Delta \tau} = \frac{A' - A}{\tau' - \tau}$, where A' , A are validation accuracies at times τ' , τ . In other words, we measure the change in accuracy over fixed periods of time. The figure reports the moving average of velocity in windows of 3 epochs (1200 iterations). In the first epoch, downsampling has a greater negative effect in validation accuracy for both models. In turn, full mode operations

Table 1: Training time reduction on CIFAR10 ($p=0.5$)

Model	error (baseline)	error (proposed)	total time reduction	iteration time reduction
ResNet-18	6.7%	6.9%	18%	63%
ResNet-50	6.3%	6.4%	23%	61%

are able to recover the model’s accuracy fairly quickly. The oscillations of $\frac{\Delta A}{\Delta \tau}$ in Figure 4 capture this phenomenon. For early training epochs (10-80) where this phenomenon is more pronounced, oscillations in ResNet50 range between $[-0.01, 0.01]$, whereas in ResNet18 they range between $[-0.08, 0.03]$ and are lopsided towards negative effects. This could imply that ResNet50 is less sensitive to the transformations performed during low-mode.

Finally, Table 1 summarizes the accuracy and training time reduction achieved with the proposed method on the two models studied. Note that the final relative error introduced by the proposed method is below 1%. As previously discussed, time savings are larger for the deeper architecture, despite the fact that per-iteration savings are similar between the two models.

5 Conclusions and Future Work

We present a method for reducing training time in CNNs with minimal impact in model accuracy. The method achieves these train-time savings by downsampling input images and kernels for a significant portion of the total number of training iterations. The method permits learning to progress even in this low-cost mode by propagating gradients from the downsampled kernels to the kernels of the target architecture that are then used to recover accuracy. For a wider application of this method, it is important to evaluate the extent to which it generalizes well for other architectures and different data regimes (e.g., Imagenet) and tasks (e.g., segmentation, detection).

References

- K. He, X. Zhang, S. Ren, and J. Sun. Deep residual learning for image recognition. In *2016 IEEE Conference on Computer Vision and Pattern Recognition (CVPR)*, pages 770–778, June 2016. doi: 10.1109/CVPR.2016.90.
- Kaiming He, Xiangyu Zhang, Shaoqing Ren, and Jian Sun. Identity mappings in deep residual networks. In Bastian Leibe, Jiri Matas, Nicu Sebe, and Max Welling, editors, *Computer Vision – ECCV 2016*, pages 630–645, Cham, 2016. Springer International Publishing. ISBN 978-3-319-46493-0.
- Christian Szegedy, Sergey Ioffe, Vincent Vanhoucke, and Alexander A. Alemi. Inception-v4, inception-resnet and the impact of residual connections on learning. In *Proceedings of the Thirty-First AAAI Conference on Artificial Intelligence, AAAI’17*, pages 4278–4284. AAAI Press, 2017. URL <http://dl.acm.org/citation.cfm?id=3298023.3298188>.
- Alex Krizhevsky, Ilya Sutskever, and Geoffrey E. Hinton. Imagenet classification with deep convolutional neural networks. *Commun. ACM*, 60(6):84–90, May 2017. ISSN 0001-0782. doi: 10.1145/3065386. URL <http://doi.acm.org/10.1145/3065386>.
- Vincent Vanhoucke, Andrew Senior, and Mark Z. Mao. Improving the speed of neural networks on cpus. In *Deep Learning and Unsupervised Feature Learning Workshop, NIPS 2011*, 2011.
- Suyog Gupta, Wei Zhang, and Fei Wang. Model accuracy and runtime tradeoff in distributed deep learning: A systematic study. In *Proceedings of the 26th International Joint Conference on Artificial Intelligence, IJCAI’17*, pages 4854–4858. AAAI Press, 2017. ISBN 978-0-9992411-0-3. URL <http://dl.acm.org/citation.cfm?id=3171837.3171972>.
- Alex Krizhevsky. One weird trick for parallelizing convolutional neural networks. *CoRR*, abs/1404.5997, 2014. URL <http://arxiv.org/abs/1404.5997>.
- Sergey Ioffe and Christian Szegedy. Batch normalization: Accelerating deep network training by reducing internal covariate shift. In *Proceedings of the 32Nd International Conference on*

- International Conference on Machine Learning - Volume 37, ICML'15*, pages 448–456. JMLR.org, 2015. URL <http://dl.acm.org/citation.cfm?id=3045118.3045167>.
- Leslie N. Smith and Nicholay Topin. Super-convergence: Very fast training of residual networks using large learning rates. *CoRR*, abs/1708.07120, 2017. URL <http://arxiv.org/abs/1708.07120>.
- Tianqi Chen, Ian J. Goodfellow, and Jonathon Shlens. Net2net: Accelerating learning via knowledge transfer. In *4th International Conference on Learning Representations, ICLR 2016, San Juan, Puerto Rico, May 2-4, 2016, Conference Track Proceedings*, 2016. URL <http://arxiv.org/abs/1511.05641>.
- Andrew Lavin. Fast algorithms for convolutional neural networks. *CoRR*, abs/1509.09308, 2015. URL <http://arxiv.org/abs/1509.09308>.
- Michaël Mathieu, Mikael Henaff, and Yann Lecun. Fast training of convolutional networks through ffts. In *International Conference on Learning Representations (ICLR2014), CBLS, April 2014*, 2014.
- Max Jaderberg, Andrea Vedaldi, and Andrew Zisserman. Speeding up convolutional neural networks with low rank expansions. In *Proceedings of the British Machine Vision Conference 2014*. British Machine Vision Association, 2014. doi: 10.5244/c.28.88. URL <https://doi.org/10.5244/2Fc.28.88>.
- Sangkug Lym, Esha Choukse, Siavash Zangeneh, Wei Wen, Mattan Erez, and Sujay Shangkavi. Prunetrain: Gradual structured pruning from scratch for faster neural network training. *CoRR*, abs/1901.09290, 2019. URL <http://arxiv.org/abs/1901.09290>.
- Jose M Alvarez and Mathieu Salzmann. Learning the number of neurons in deep networks. In D. D. Lee, M. Sugiyama, U. V. Luxburg, I. Guyon, and R. Garnett, editors, *Advances in Neural Information Processing Systems 29*, pages 2270–2278. Curran Associates, Inc., 2016. URL <http://papers.nips.cc/paper/6372-learning-the-number-of-neurons-in-deep-networks.pdf>.
- Pedro Porto Buarque de Gusmão, Gianluca Francini, Skjalg Lepsøy, and Enrico Magli. Fast training of convolutional neural networks via kernel rescaling. *CoRR*, abs/1610.03623, 2016. URL <http://arxiv.org/abs/1610.03623>.
- Jason Kuen, Xiangfei Kong, Lin Zhe, Gang Wang, Jianxiong Yin, Simon See, and Yap-Peng Tan. Stochastic downsampling for cost-adjustable inference and improved regularization in convolutional networks. *IEEE/CVF Conference on Computer Vision and Pattern Recognition (CVPR)*, 2018.
- Mingxing Tan and Quoc V. Le. Efficientnet: Rethinking model scaling for convolutional neural networks. 05 2019.
- Surat Teerapittayanon, Bradley McDanel, and H.T. Kung. BranchyNet: Fast inference via early exiting from deep neural networks. In *2016 23rd International Conference on Pattern Recognition (ICPR)*. IEEE, dec 2016. doi: 10.1109/icpr.2016.7900006. URL <https://doi.org/10.1109/2Ficpr.2016.7900006>.
- Patryk Chrabaszcz, Ilya Loshchilov, and Frank Hutter. A downsampled variant of imagenet as an alternative to the CIFAR datasets. *CoRR*, abs/1707.08819, 2017. URL <http://arxiv.org/abs/1707.08819>.
- Geoffrey E. Hinton, Oriol Vinyals, and Jeffrey Dean. Distilling the knowledge in a neural network. *CoRR*, abs/1503.02531, 2015.
- David E. Rumelhart, Geoffrey E. Hinton, and Ronald J. Williams. Neurocomputing: Foundations of research. chapter Learning Representations by Back-propagating Errors, pages 696–699. MIT Press, Cambridge, MA, USA, 1988. ISBN 0-262-01097-6. URL <http://dl.acm.org/citation.cfm?id=65669.104451>.
- Mark Nixon and Alberto S. Aguado. *Feature Extraction & Image Processing, Second Edition*. Academic Press, Inc., Orlando, FL, USA, 2nd edition, 2008. ISBN 0123725380, 9780123725387.

Alex Krizhevsky. Learning multiple layers of features from tiny images. *University of Toronto*, 05 2012.